



MCNP analysis and optimization of a double crystal phoswich detector

I- Introduction.....	3
II- Monte Carlo method and MCNPX code.....	3
III- Properties and geometrical characteristics of the scintillators.....	4
IV- Comparison of the MCNPX and GEANT4 responses	6
V- Study of scintillators response in the case of photons	7
VI- Study of scintillators response in the case of protons.....	16
VI-1 LaBr ₃ :Ce response	17
VI-2 LaCl ₃ :Ce response	20
VI-3 LYSO response	23
VI-4 The phoswich of (LaBr ₃ :Ce, LaCl ₃ :Ce) response.....	26
VII- Conclusion.....	28
IX-References.....	28

I- Introduction

Since the discovery of LaCl₃:Ce, LaBr₃:Ce and LYSO scintillators, several groups have furthered understanding of their properties. In this work, we are going to study the response of BrillianceTM380, BrillianceTM350 and Prelude 420 scintillators for photons at energy range from 0 up to 20 MeV and for protons from 0 up to 150 MeV. The study aims to develop a double crystal phoswich detector, with high space energy resolution and high sensibility, where two different crystals must be connected to the same photomultiplier. The study consists of using MCNPX and GEANT4 computer codes based both on the Monte Carlo method.

II- Monte Carlo method and MCNPX code

MCNPX (Monte Carlo N-Particle eXtended), is a general purpose Monte Carlo radiation transport code for modelling the interaction of radiation with materials. MCNPX is fully three-dimensional and it utilizes the latest nuclear cross section libraries and uses physics models for particle types and energies where tabular data are not available. MCNPX is used for nuclear medicine, nuclear safeguards, accelerator applications, nuclear criticality and much more.

In the Monte Carlo process, the solution is obtained by calculating random particle histories. In each history the random walk is based on the particle cross section libraries and geometrical information. Each particle ceases to exit or is, somehow, transferred outside the problem range. In order to achieve a statistically reasonable and accurate result, the number of particle history simulations that are considered has to be fairly large. This generally requires a powerful computer. An important consideration is to use the correct variance reduction technique in Monte Carlo simulations to shorten CPU time without decreasing the accuracy of the result.

The detector geometry is modelled with the MCNPX code, which allows simulating physical events occurring during the detection and registers them to build energy spectrum. The code is suitable for modelling the detector response by means of its pulse height tally F8. This tally which provides the energy distribution of pulses created in a detector by radiation. The net response is a spectrum of pulses with heights proportional to the frequency of events in distinct energy bins.

III- Properties and geometrical characteristics of the scintillators

Table 1, summarizes the properties of Brilliance380, Brilliance350 and Prelude420 scintillators. All the data presented in this table were taken from the **Saint Gobain technical note (revision: October, 2007)**.

Table 1: Scintillators properties

Scintillator	Light Yield (ph./keV)	1/e decay time (ns)	F.O.M $\sqrt{t/LY}$	Wavelength of maximum emission λ_m (mm)	Refractive index at λ_m	Density (g/cm ³)	Thickness (cm) for 50% attenuation (662keV)
NaI(Tl)	38	250	2.6	415	1.85	3.67	2.5
Brilliance TM 350	49	28	0.8	350	~1.9	3.85	2.3
Brilliance TM 380	63	16	0.5	380	~1.9	5.08	1.8
Prelude TM 420	32	41	1.1	420	1.81	7.1	1.1

The models simulated are Teflon reflected cylinders of 20mm of diameter. The thicknesses studied are respectively 50mm for Brilliance350 and Prelude420 and 30mm for Brilliance380. Study was also carried for a phoswich of Brilliance350 and Brilliance380 cylinders of 50mm and 30mm of thickness respectively. The individual B350 and B380 scintillators are coupled to a glass light guide of 20mm in diameter and 5mm thick. These scintillators are all surrounded by 0.5mm of Aluminium. Figures 1 to 4 show the MCNP geometry construction of the four models studied.

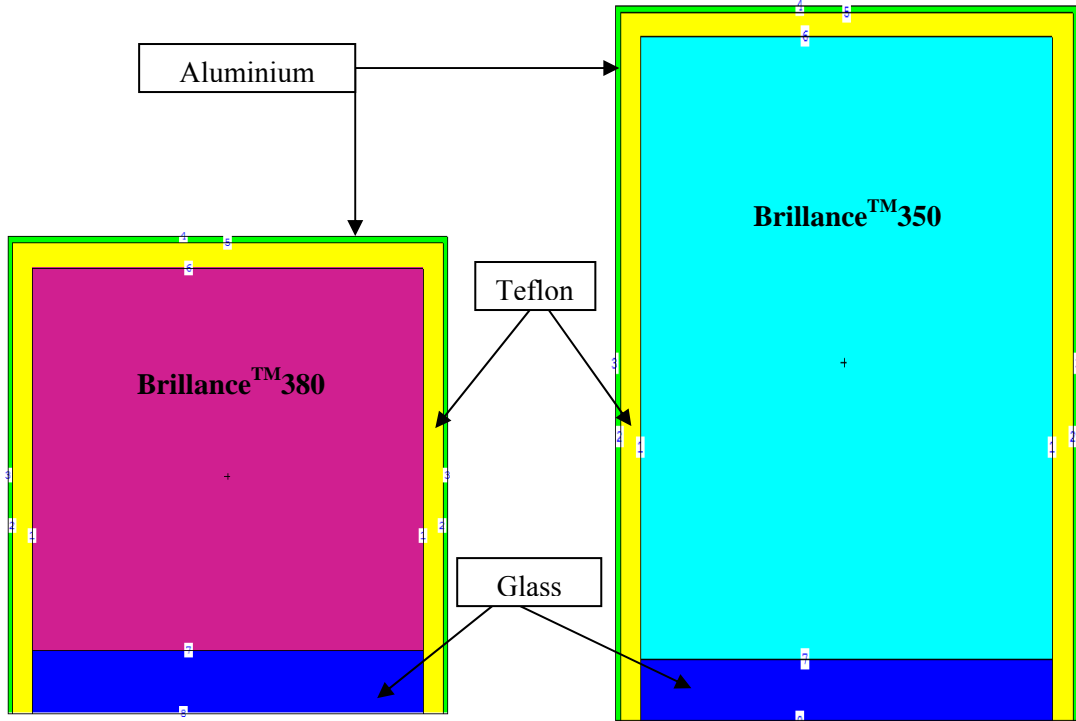


Fig. 1: XZ view of Brilliance 380 detector.

Fig. 2: XZ view of Brilliance 350 detector.

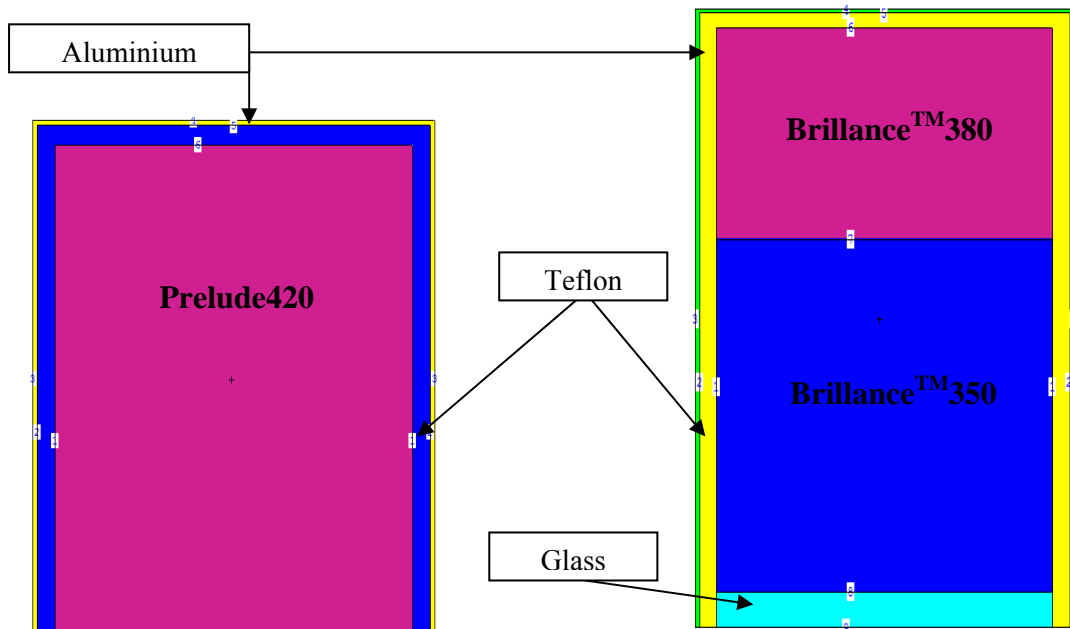


Fig. 3: XZ view of Prelude420 detector.

Fig. 4: XZ view for a phoswich of Brilliance380 and Brilliance350.

IV- Comparison of the MCNPX and GEANT4 responses

Because of a lack of accurate experimental measurements, a comparison between the results of the two Monte Carlo codes MCNPX and GEANT4 has been carried. The study consists of simulating a set of 3"x3" and 1"x1" LaBr₃:Ce and LYSO cylindrical scintillators and comparing the peak to total values obtained by the two codes as a function of photon incident energies.

Figures 5 and 6, represent the results of simulation obtained for LaBr₃:Ce and LYSO scintillators respectively.

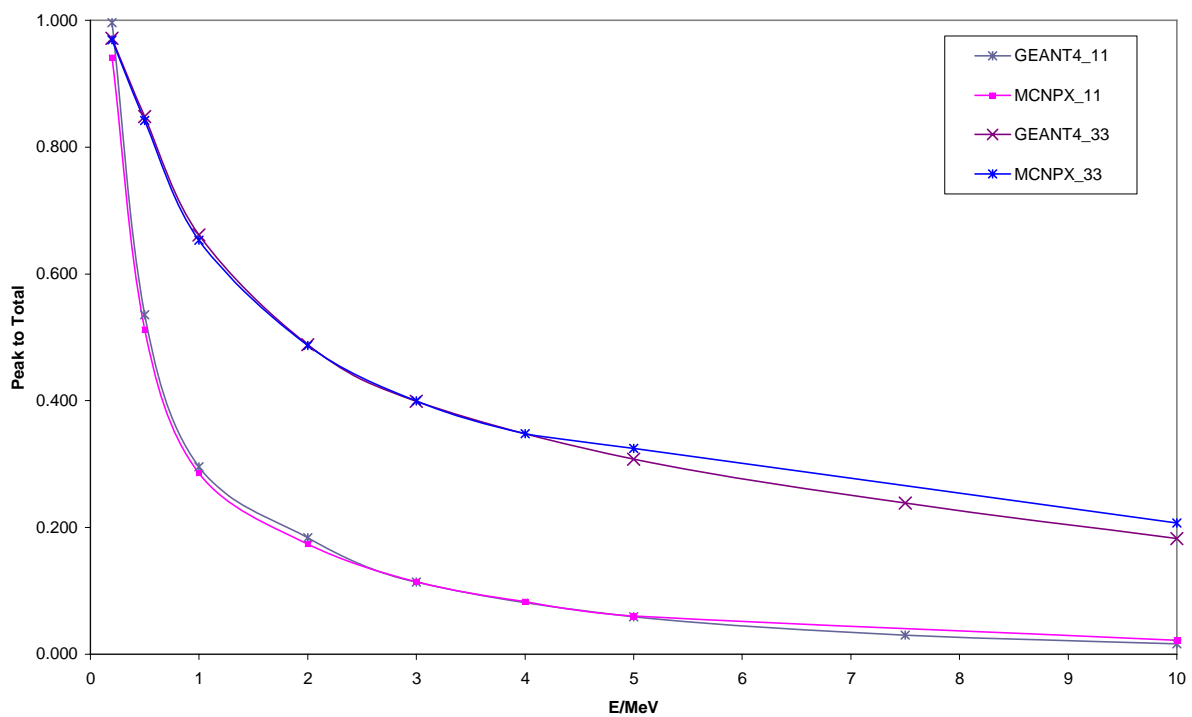


Fig. 5: Peak to total versus photon energy obtained by MCNPX and GEANT4 for 1"x1" and 3"x3" cylinders of Brilliance™380.

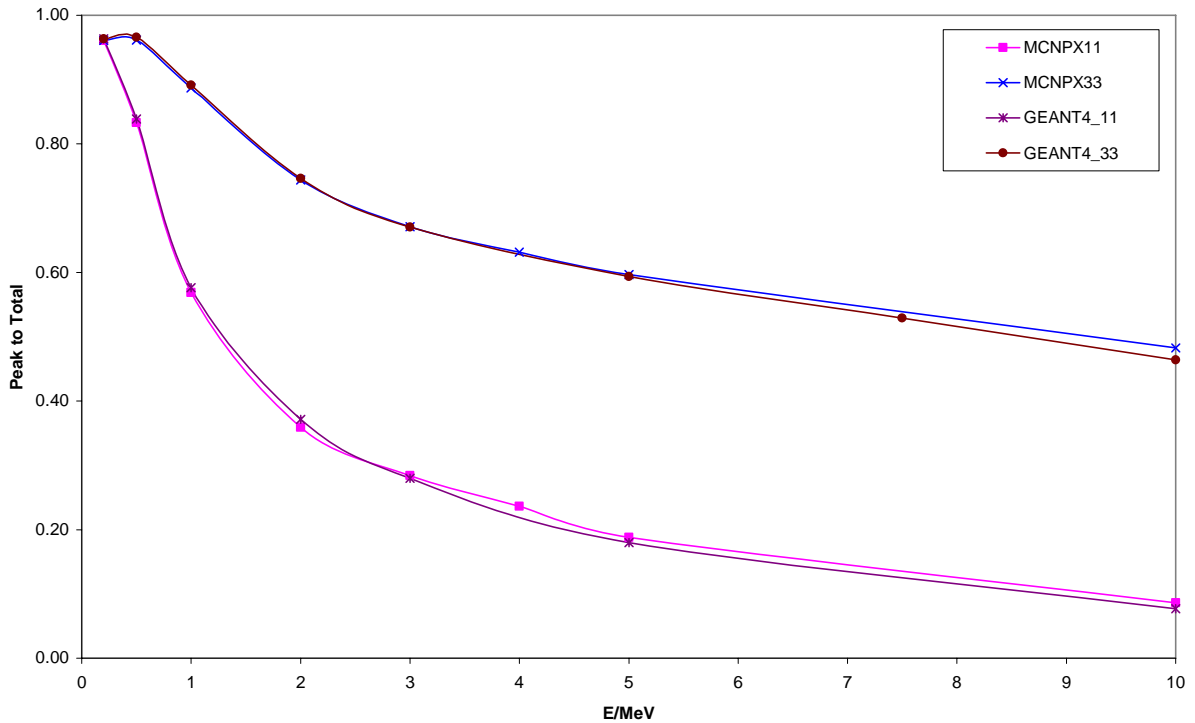


Fig. 6: Peak to total versus energy obtained by MCNPX and GEANT4 for 1”x1” and 3”x3” cylinders of PreludeTM420.

According to the figures above, we remark a well agreement between the MCNPX and GEANT4 calculated peak to total values, especially for energy range lower than 5MeV. The small differences existing for high energies ($>5\text{MeV}$) can be attributed to the difference between the cross sections libraries used by the two codes.

V- Study of scintillators response in the case of photons

In this part, we represent the gamma study for BrillianceTM380, BrillianceTM350, PreludeTM420 and a phoswich detector of BrillianceTM380 and BrillianceTM350 (figures 1 to 4). We have calculated the peak to total values for an energy range going from 0 to 20 MeV, and the energy spectrums for each scintillator. The source was located at 10 cm from the upper surface of each detector and the emission was monodirectional crossing perpendicularly the centre of detectors. The energy resolutions for ^{137}Cs (662keV) for B380, B350 and P420 respectively are 2.9%, 3.8%, 7.1%.

Figures 7 to 10, show the peak to total versus energy curves calculated by MCNPX code for the four detectors described above.

On figures 11 to 22, we represent the energy spectra calculated by MCNPX code for the same detectors.

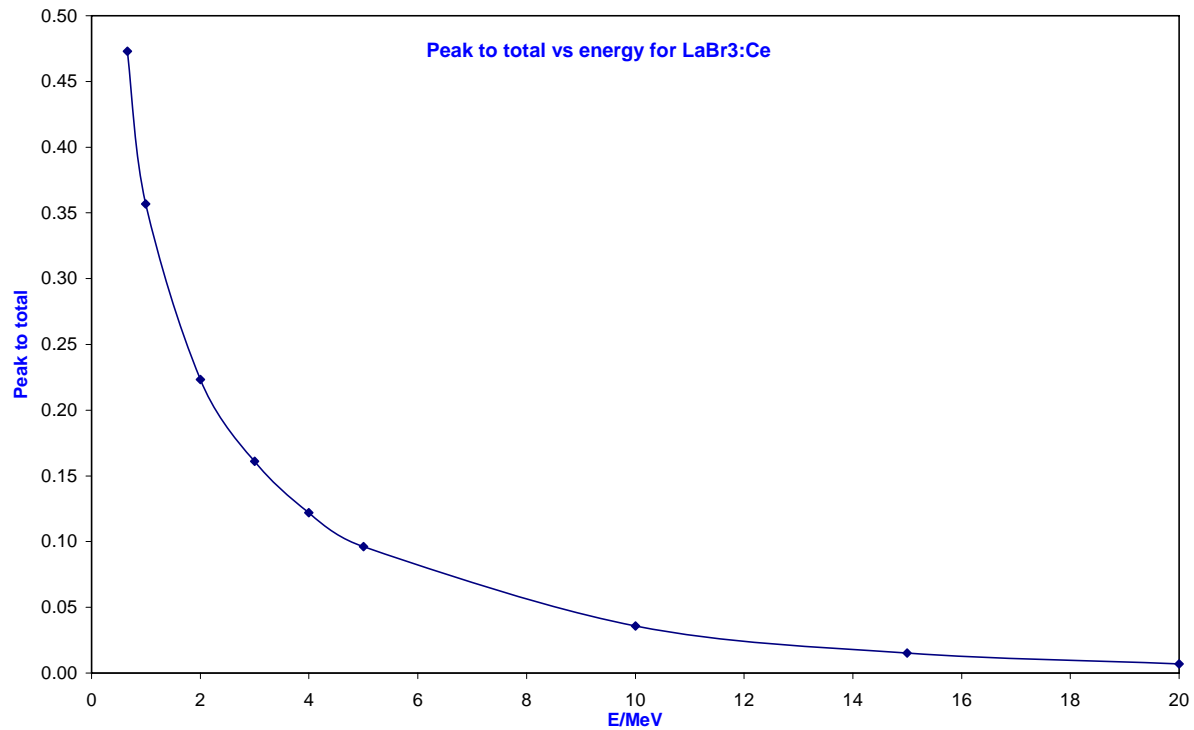


Fig. 7: Peak to total versus energy calculated by MCNPX for LaBr₃:Ce scintillator.

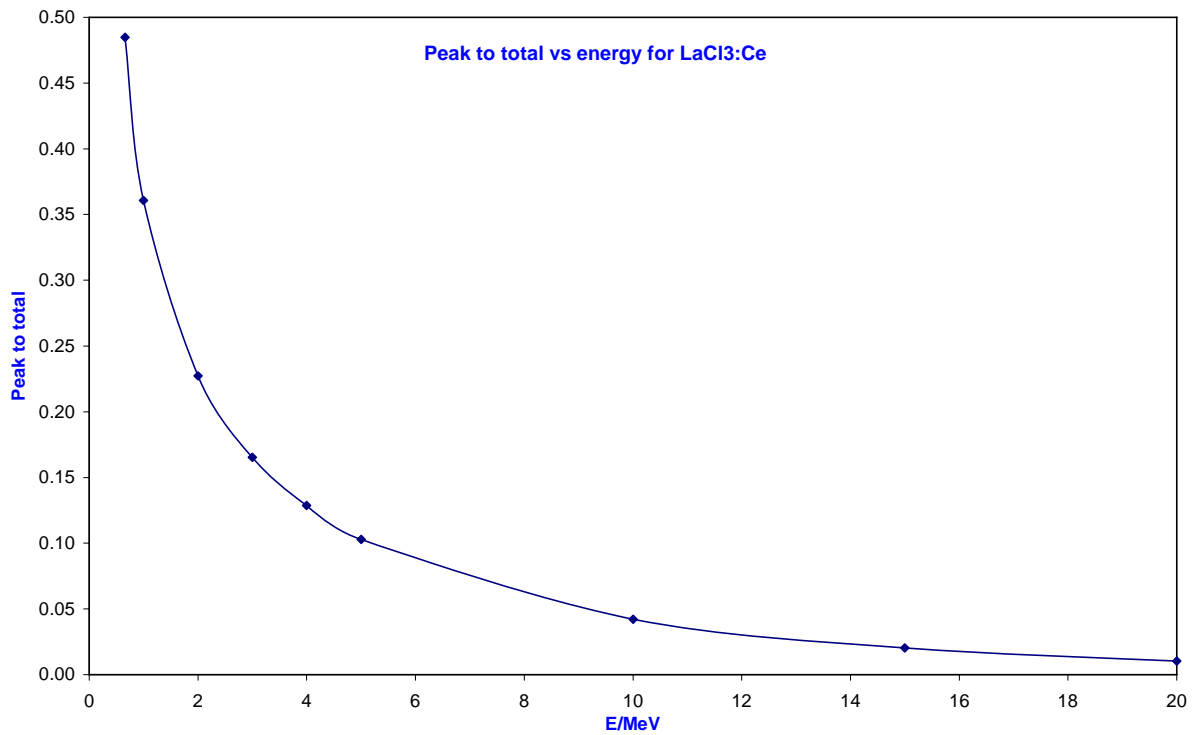


Fig. 8: Peak to total versus energy calculated by MCNPX for LaCl₃:Ce scintillator.

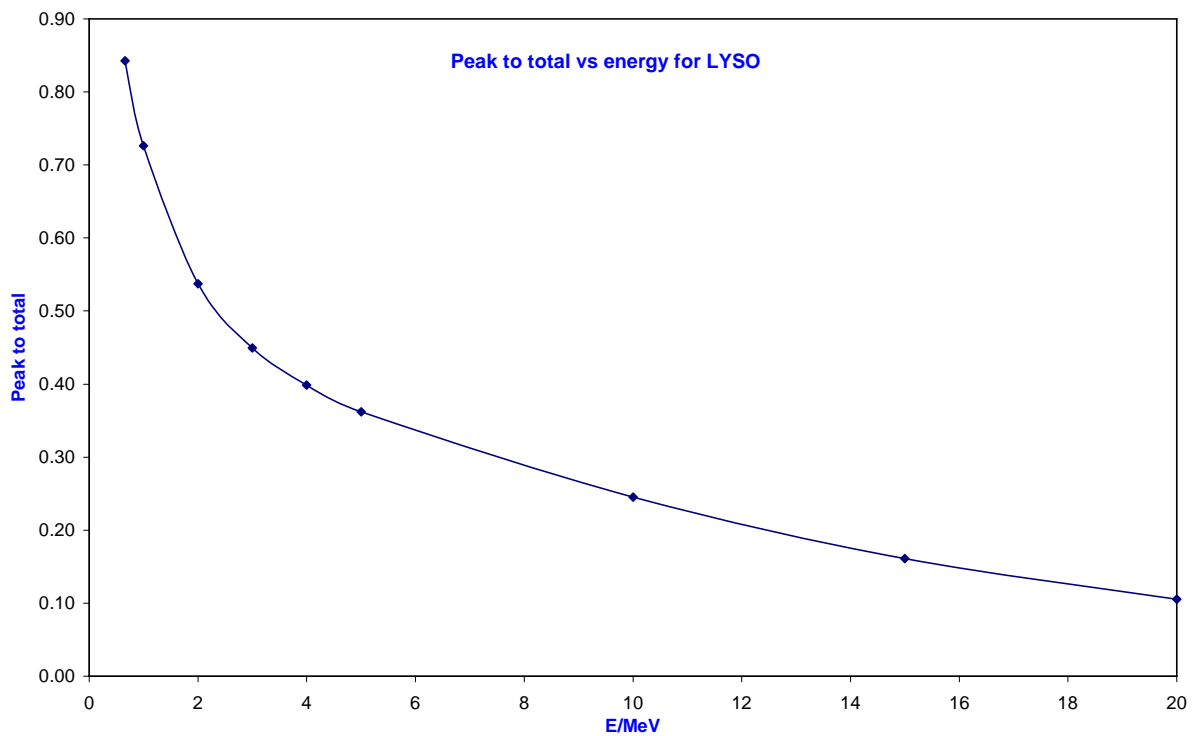


Fig. 9: Peak to total versus energy calculated by MCNPX for LYSO scintillator.

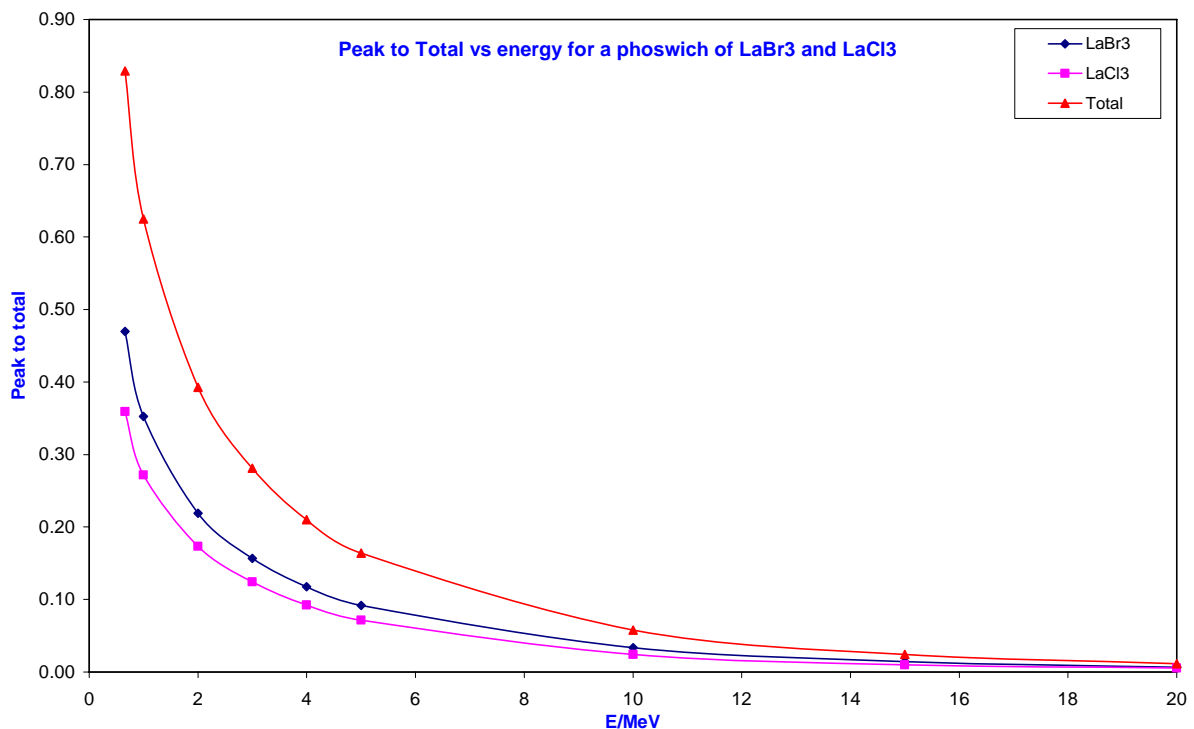


Fig. 10: Peak to total versus energy calculated by MCNPX for a phoswich of LaBr₃:Ce and LaCl₃:Ce.

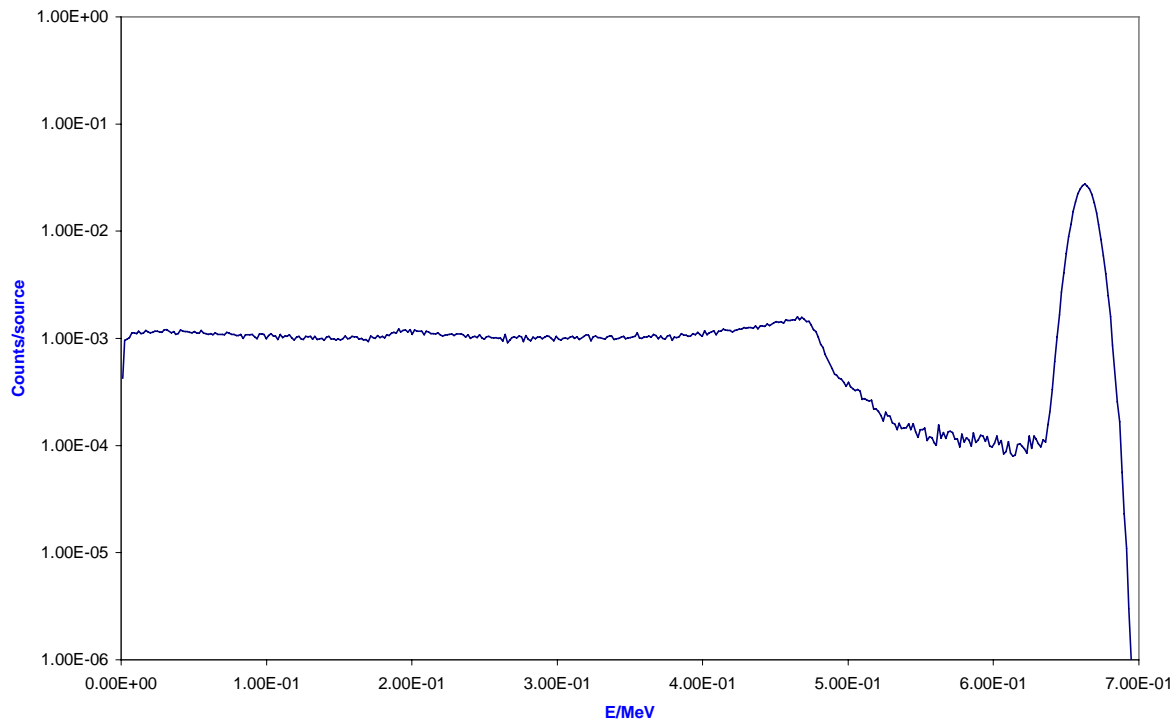


Fig. 11: Energy spectrum calculated by MCNPX for LaBr₃:Ce at 662keV.

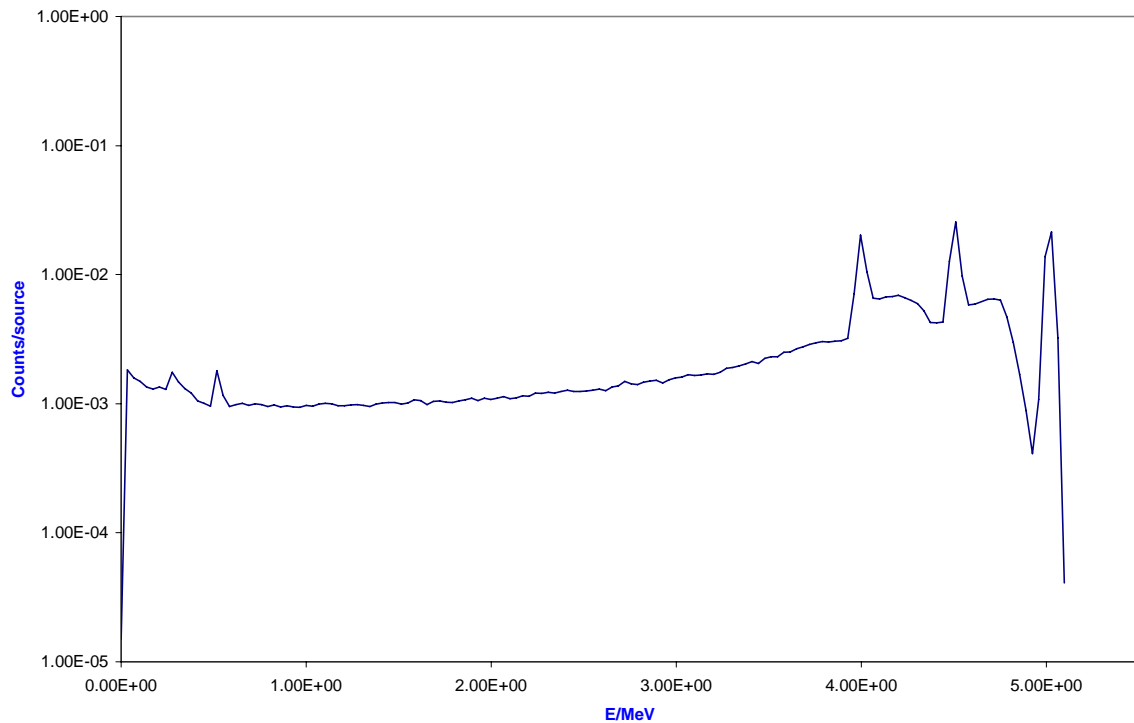


Fig. 12: Energy spectrum calculated by MCNPX for LaBr₃:Ce at 5MeV.

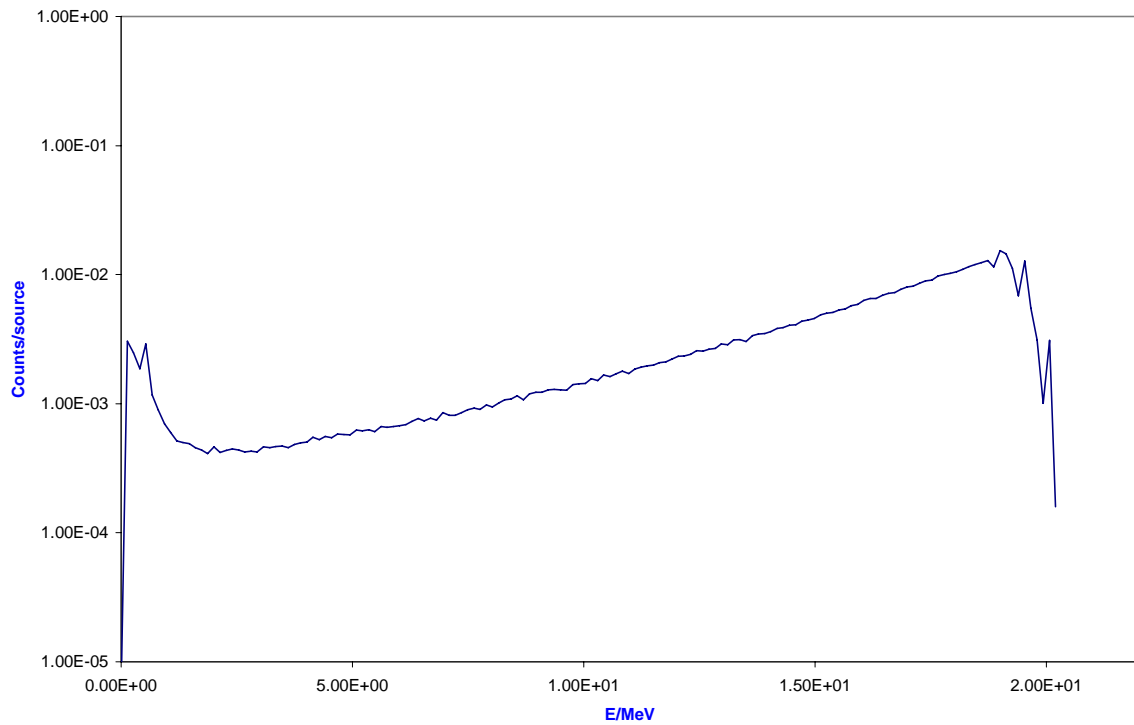


Fig. 13: Energy spectrum calculated by MCNPX for LaBr₃:Ce at 20MeV.

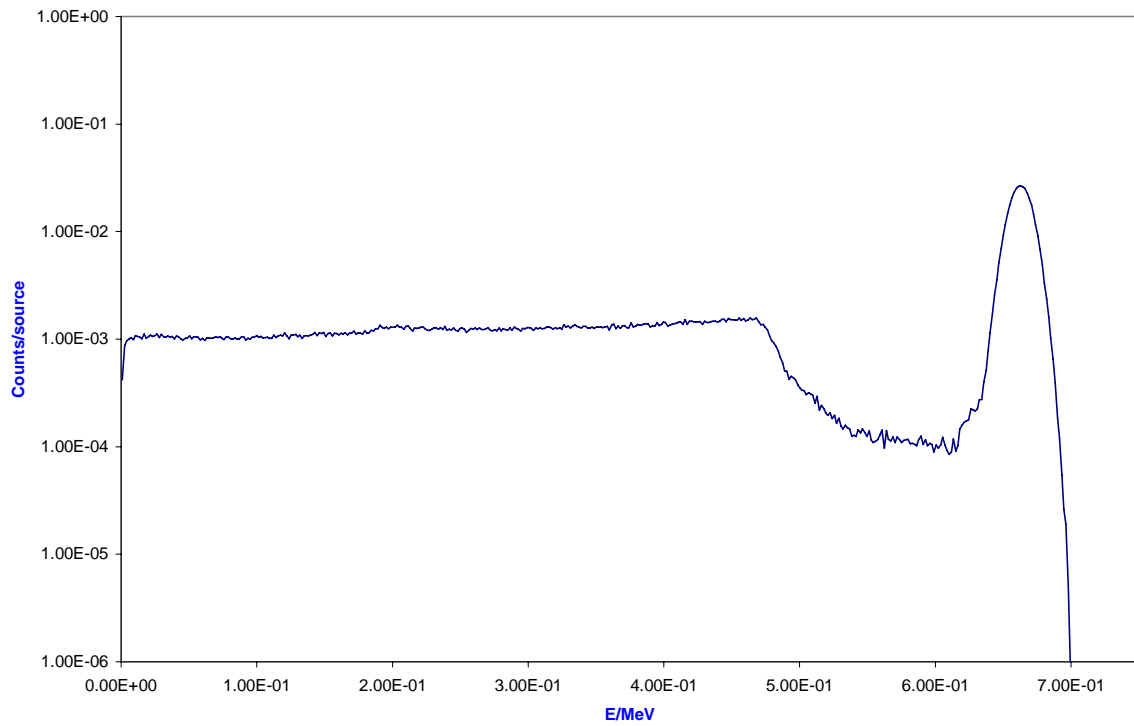


Fig. 14: Energy spectrum calculated by MCNPX for LaCl₃:Ce at 662keV.

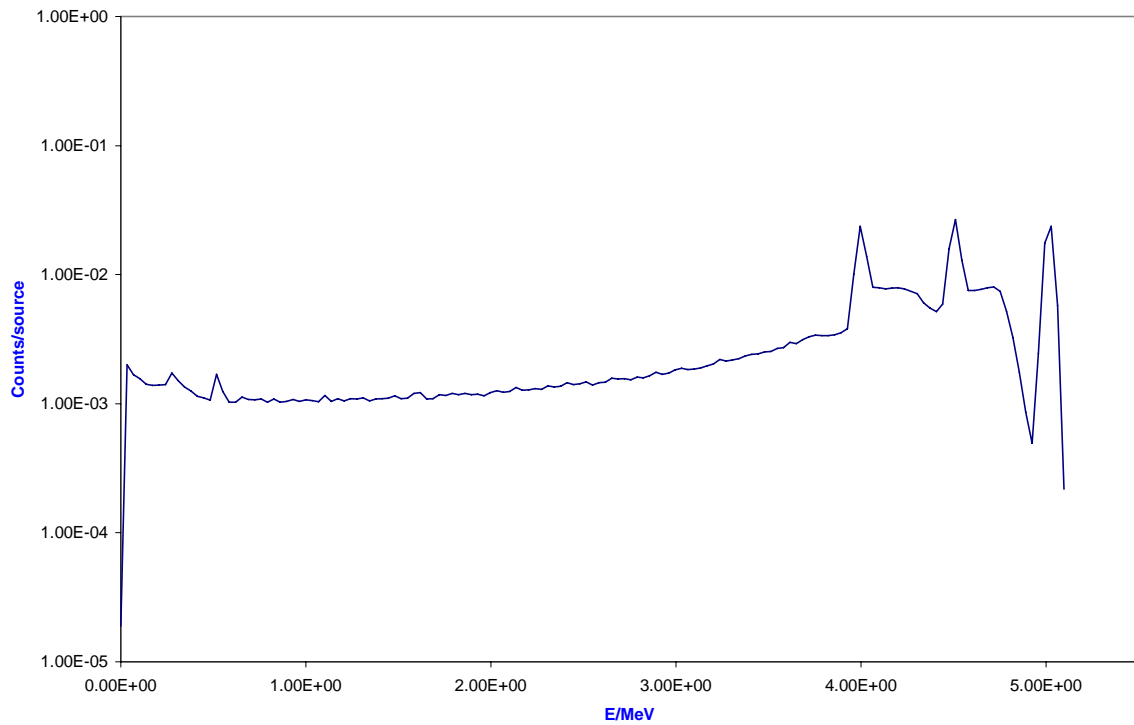


Fig. 15: Energy spectrum calculated by MCNPX for LaCl₃:Ce at 5MeV.

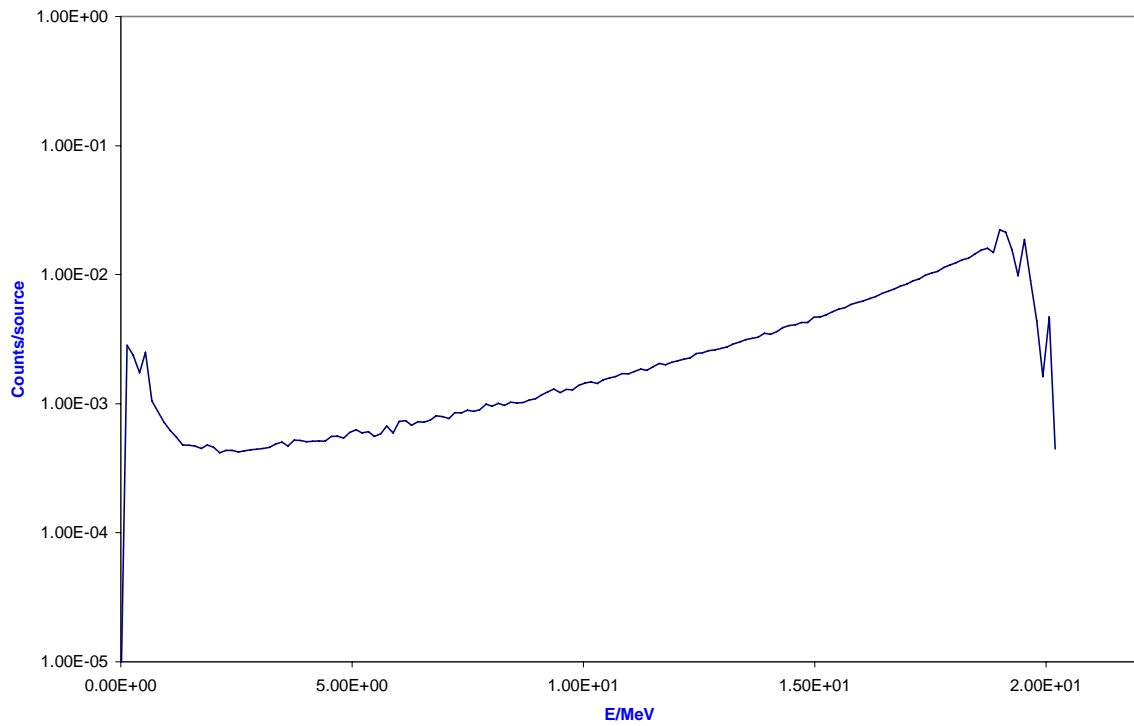


Fig. 16: Energy spectrum calculated by MCNPX for LaCl₃:Ce at 20MeV.

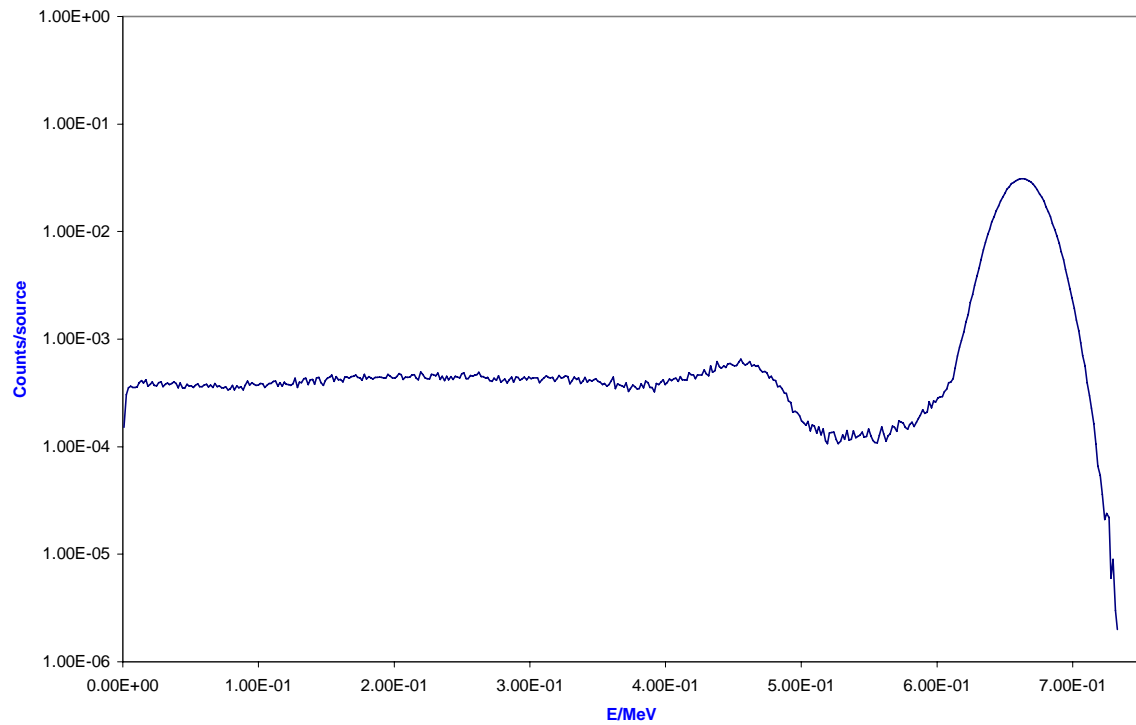


Fig. 17: Energy spectrum calculated by MCNPX for LYSO at 662keV.

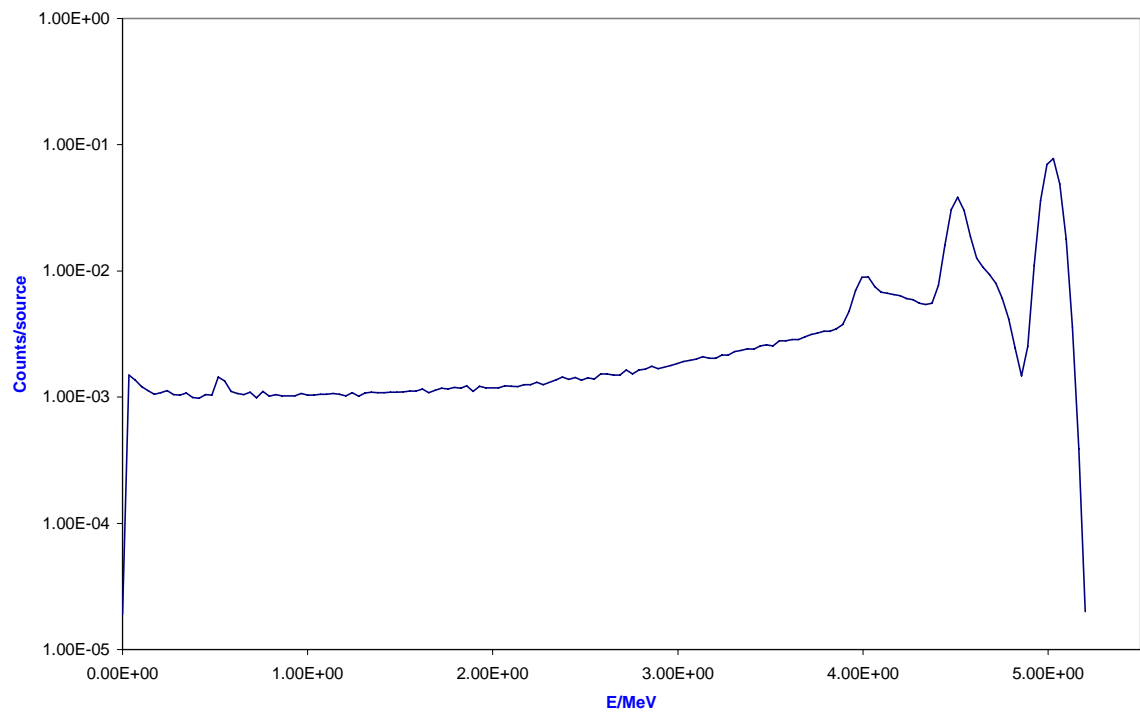


Fig. 18: Energy spectrum calculated by MCNPX for LYSO at 5MeV.

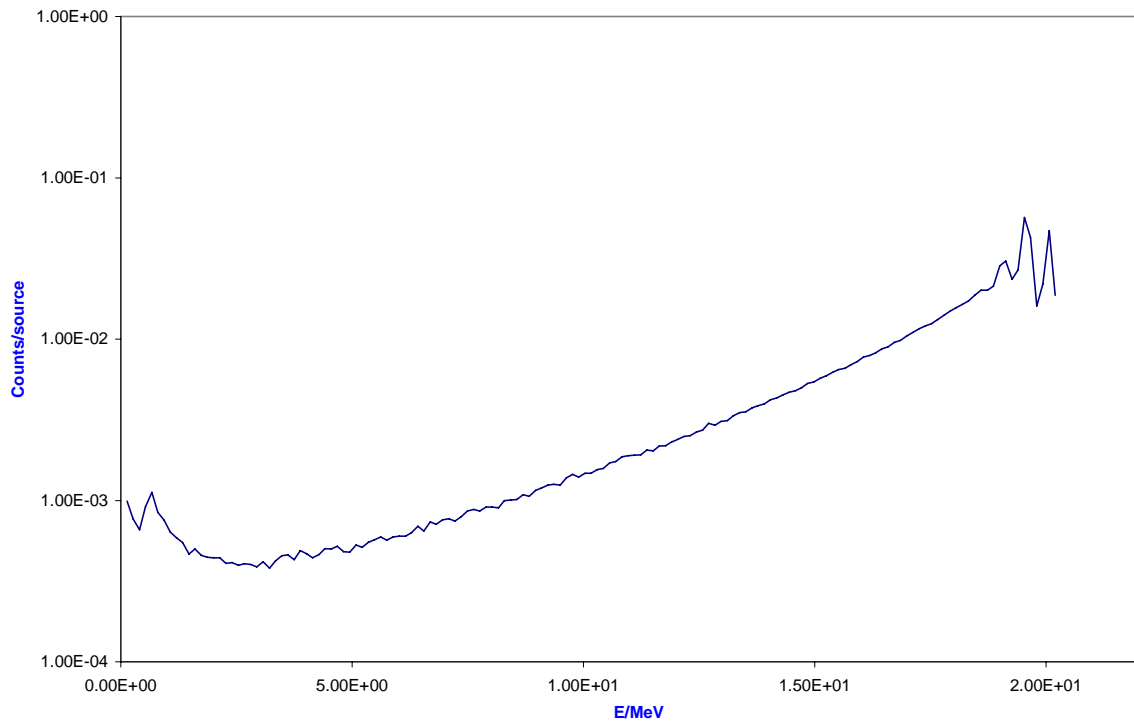


Fig. 19: Energy spectrum calculated by MCNPX for LYSO at 20MeV.

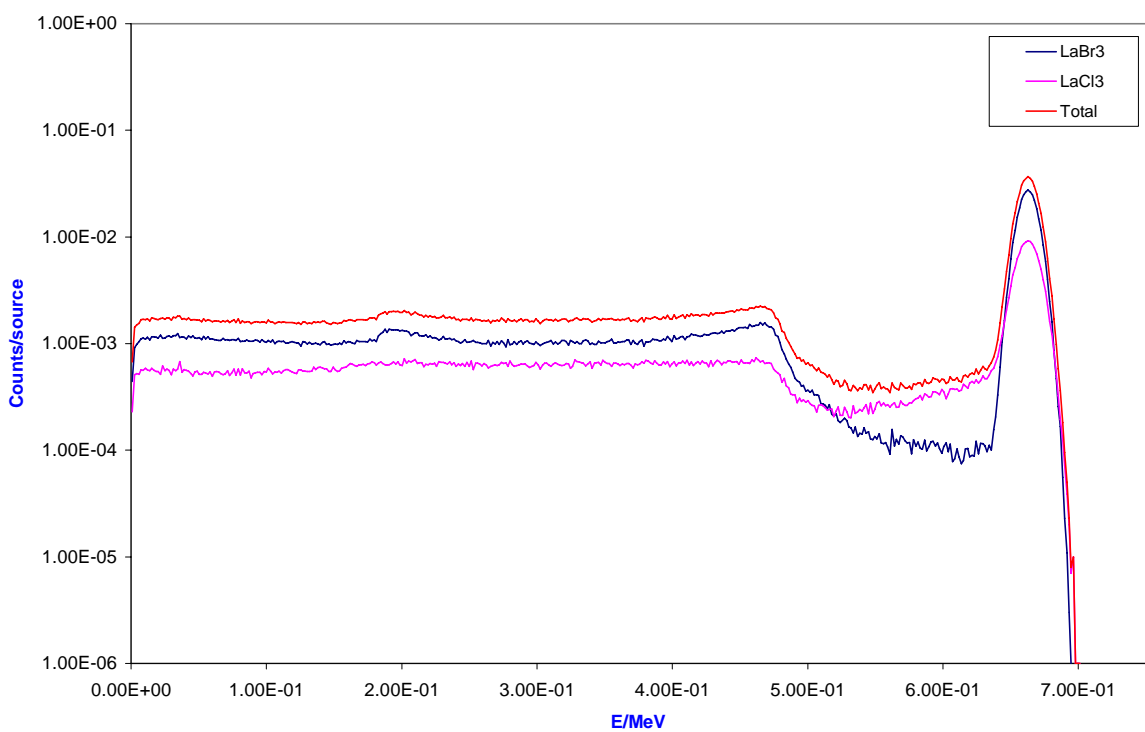


Fig. 20: Energy spectra calculated by MCNPX for a phosphwich of Brillance™380 and Brillance™350 at 662keV.

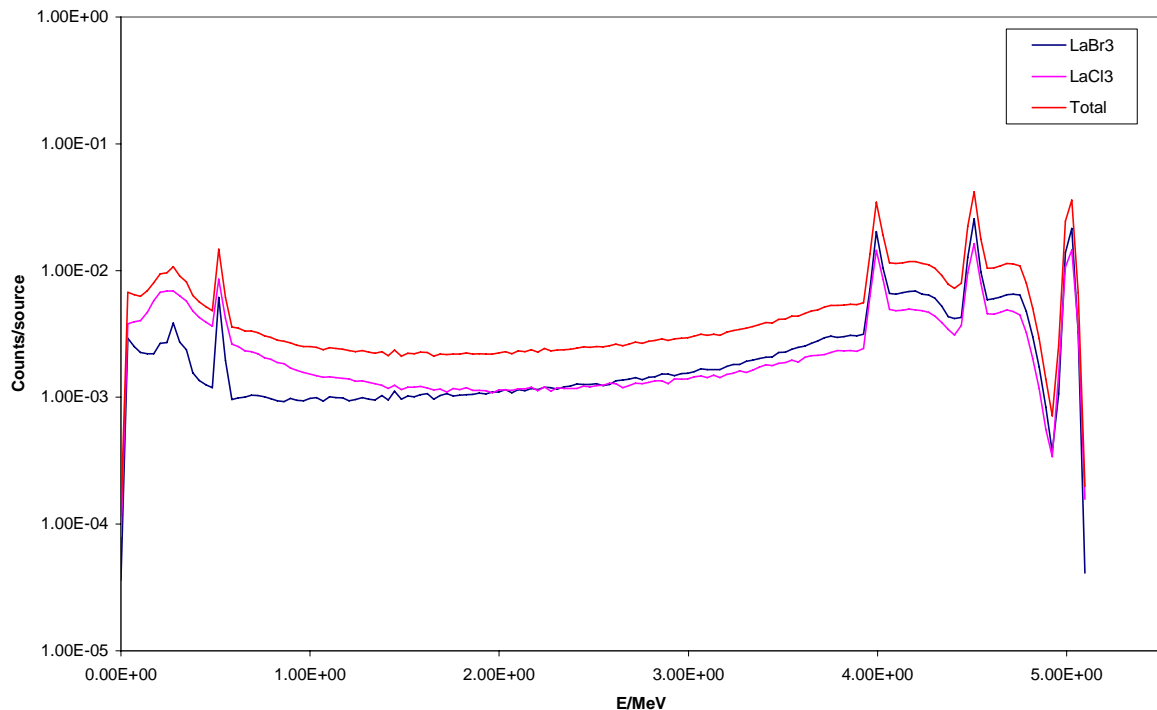


Fig. 21: Energy spectra calculated by MCNPX for a phoswich of BrillianceTM380 and BrillianceTM350 at 5MeV.

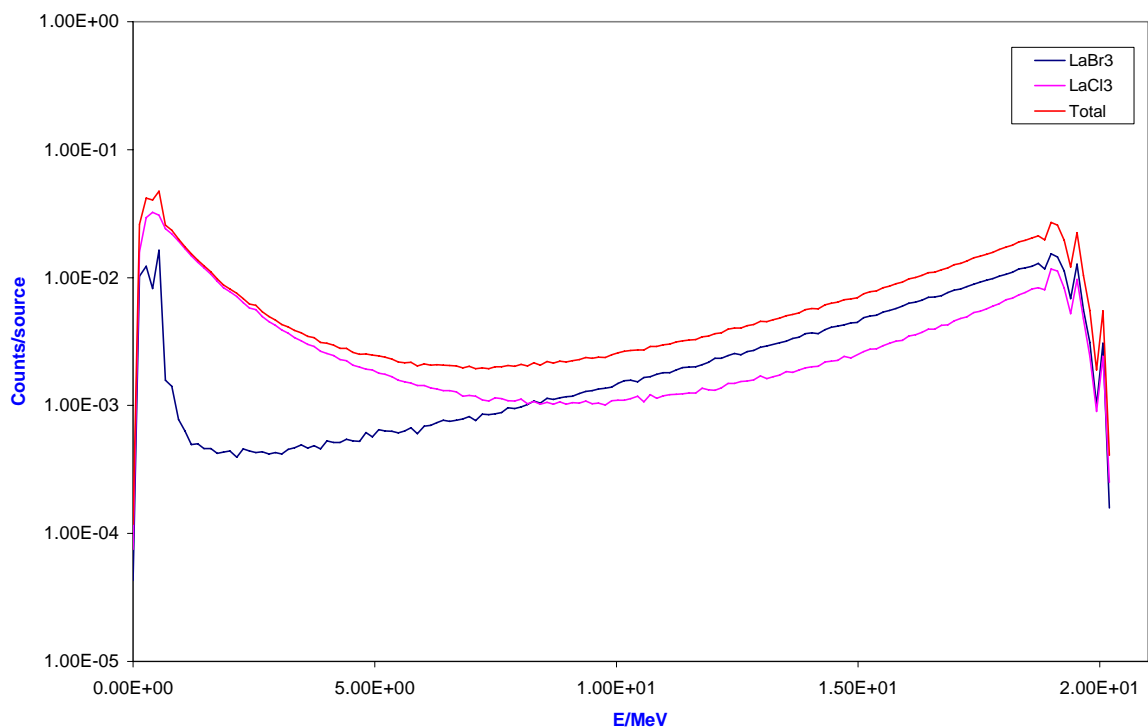


Fig. 22: Energy spectra calculated by MCNPX for a phoswich of BrillianceTM380 and BrillianceTM350 at 20MeV.

VI- Study of scintillators response in the case of protons

This study concerns the behaviour of LaBr₃:Ce, LaCl₃:Ce (individually and phoswich) and LYSO versus proton beam energy (up to 150MeV). In our Monte Carlo simulations, we have used the same scintillators described in third paragraph of this report, the study consists of calculating, by means of MCNPX code, the total proton energy deposited in each scintillator, also we have calculated the average track mean free path (mfp), and energy spectra in all the studied cases.

We have remarked that, the 0.5mm layer of Teflon existing at the entrance of the scintillators bans protons with lower than 20MeV to enter into the scintillators. Protons of energy ranging from 30 to 100MeV deposit 34% to 4% of their energy on the first layer of Teflon and the rest is deposited inside the crystals. For proton of energies higher than 100MeV, we remark that an important fraction of protons escapes from the individual scintillators. This fraction increases with the incident proton energy. Tables below, give more detailed results.

Table 2: Energy deposition and average track mean free path versus incident energy for LaBr₃:Ce.

E(MeV)	Energy deposition (MeV)	average Track mfp (cm)
30	19.61	1.53E-03
50	43.42	6.06E-03
70	64.89	1.22E-02
100	95.74	2.40E-02
120	83.71	3.74E-02
150	65.85	6.82E-02

Table 3: Energy deposition and the average track mean free path versus incident energy for LaCl₃:Ce.

E(MeV)	Energy deposition (MeV)	average Track mfp (cm)
30	19.61	1.82E-03
50	43.42	7.31E-03
70	64.89	1.47E-02
100	95.72	2.91E-02
120	115.91	4.06E-02
150	95.51	7.11E-02

Table 4: Energy deposition and the average track mean free path versus incident energy for LYSO.

E(MeV)	Energy deposition (MeV)	average Track mfp (cm)
30	19.63	8.75E-04
50	43.49	3.45E-03
70	65.01	6.93E-03
100	95.97	1.36E-02
120	116.34	1.90E-02
150	146.61	2.81E-02

Table 5: Energy deposition and the average track mean free path versus incident energy for a phoswich of LaBr₃:Ce and LaCl₃:Ce.

E(MeV)	LaBr ₃ :Ce		LaCl ₃ :Ce	
	Energy deposition (MeV)	average Track mfp (cm)	Energy deposition (MeV)	average Track mfp (cm)
30	19.61	1.53E-03	0.00	-
50	43.42	6.06E-03	0.00	-
70	64.89	1.22E-02	0.00	-
100	95.74	2.40E-02	0.01	-
120	83.71	3.74E-02	32.30	5.36E-03
150	65.85	6.82E-02	80.01	2.51E-02

VI-1 LaBr₃:Ce response

The figures below show the energy spectra calculated by MCNPX code for BrillianceTM380 scintillator for different proton energy sources.

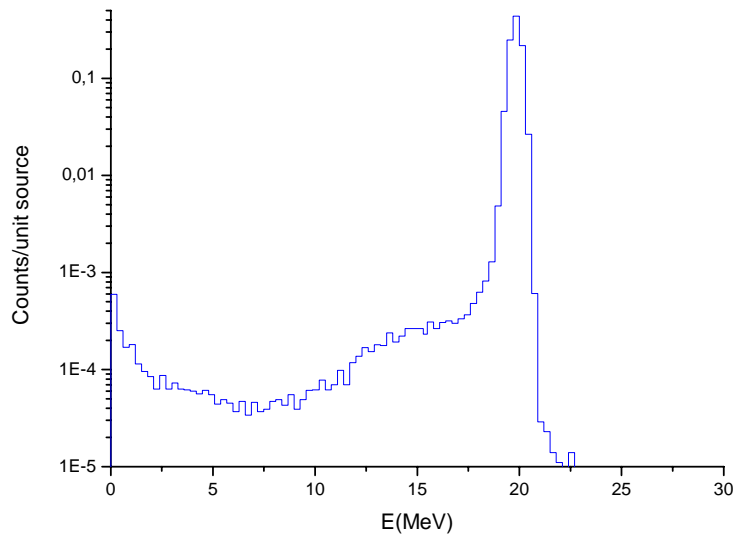


Fig. 23: Energy spectrum of LaBr₃:Ce for 30MeV protons.

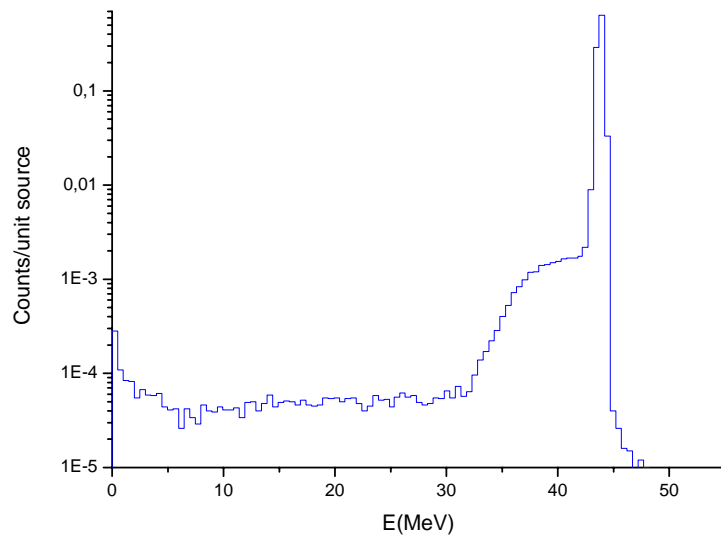


Fig. 24: Energy spectrum for LaBr₃:Ce at 50MeV.

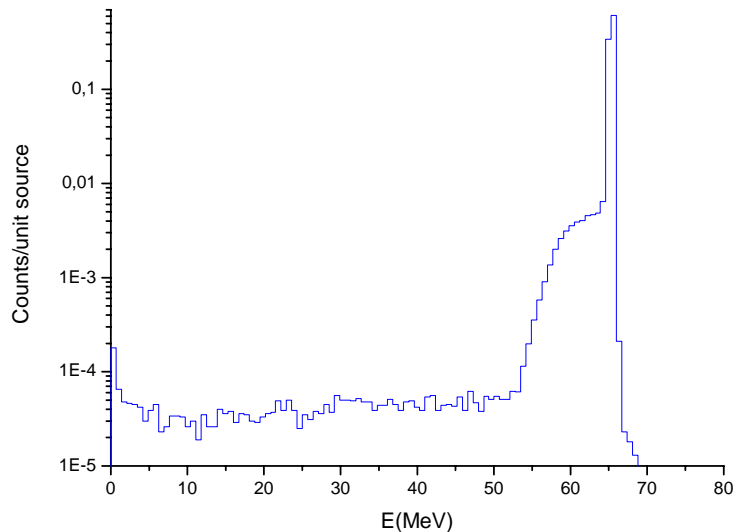


Fig. 25: Energy spectrum of LaBr₃:Ce for 70MeV protons.

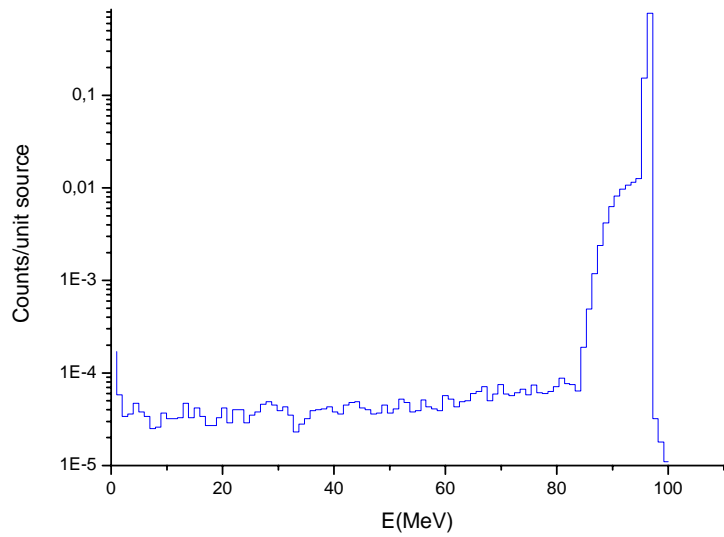


Fig. 26: Energy spectrum of LaBr₃:Ce for protons of 100MeV.

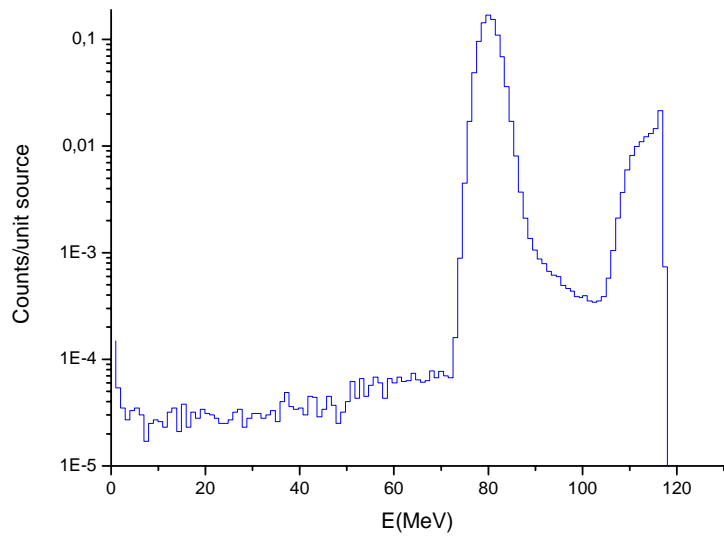


Fig. 27: Energy spectrum of LaBr₃:Ce for protons of 120MeV.

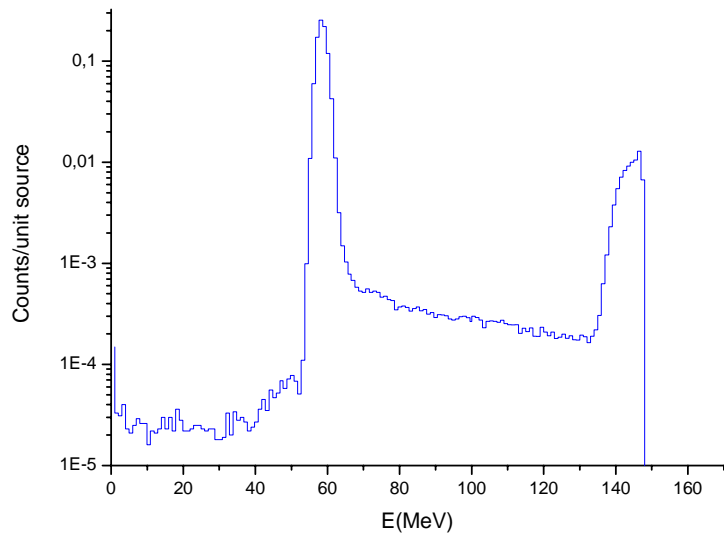


Fig. 28: Energy spectrum of LaBr₃:Ce for protons of 150MeV.

VI-2 LaCl₃:Ce response

The following figures show the energy spectra as calculated by MCNPX code for BrillianceTM350 scintillator for different proton energies.

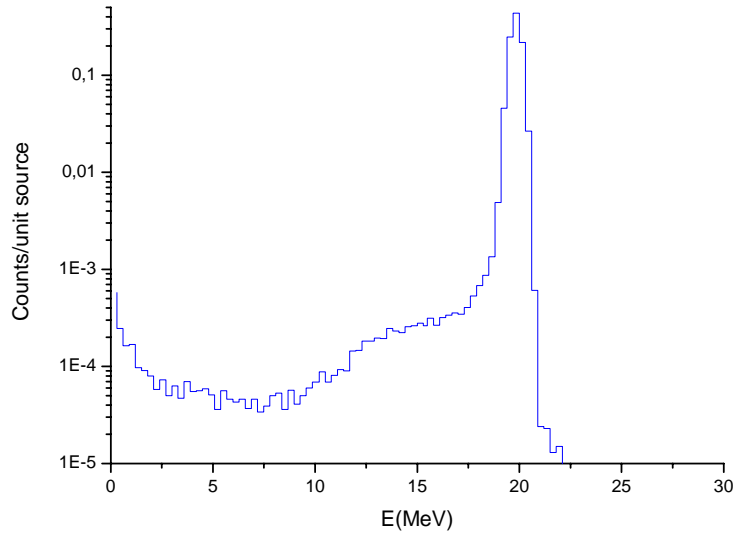


Fig. 29: Energy spectrum of LaCl₃:Ce for 30MeV protons.

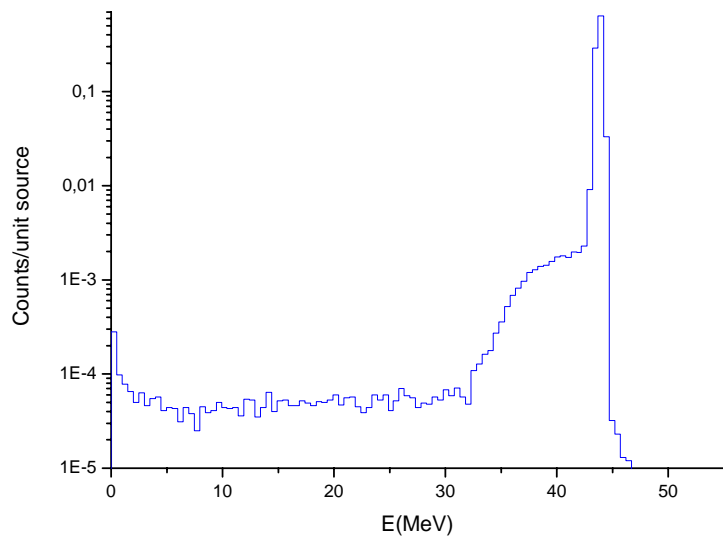


Fig. 30: Energy spectrum of LaCl₃:Ce for 50MeV protons.

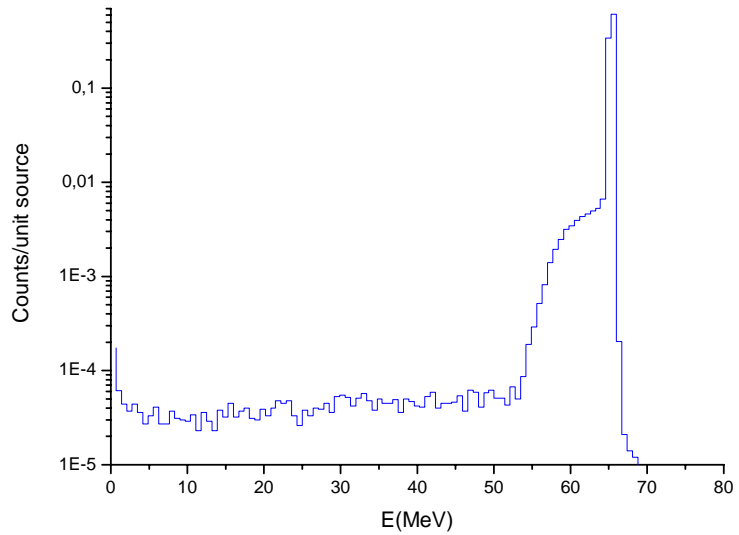


Fig. 31: Energy spectrum of LaCl₃:Ce for protons of 70MeV.

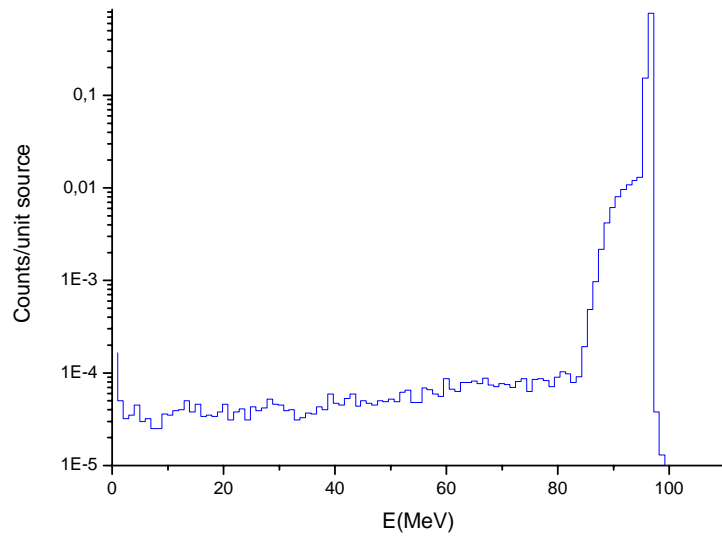


Fig. 32: Energy spectrum of LaCl₃:Ce for 100MeV protons.

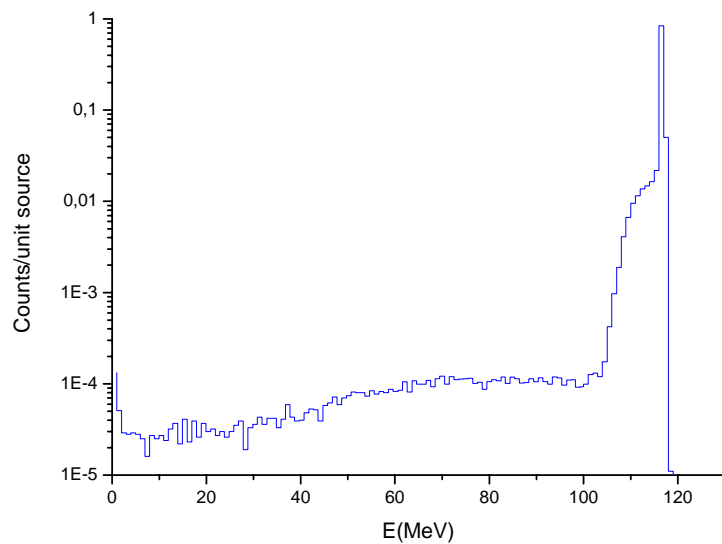


Fig. 33: Energy spectrum of LaCl₃:Ce for protons of 120MeV.

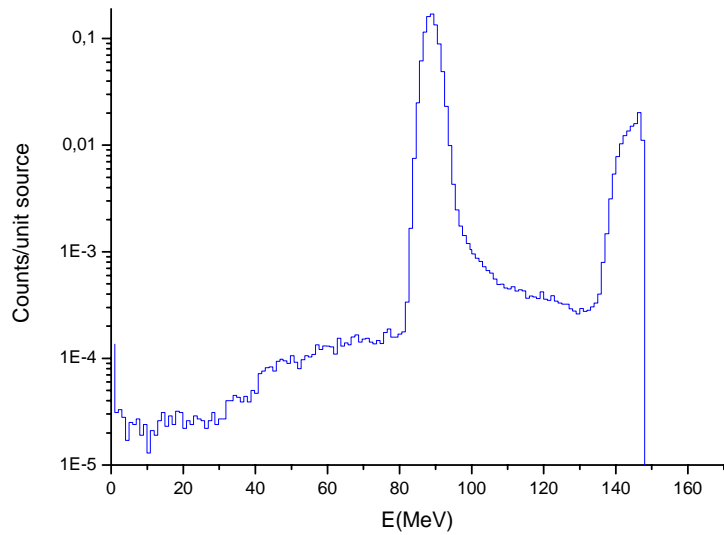


Fig. 34: Energy spectrum of LaCl₃:Ce for protons of 150MeV.

VI-3 LYSO response

The figures below give the energy spectra produced by MCNPX code for PreludeTM420 scintillator and different proton energy sources.

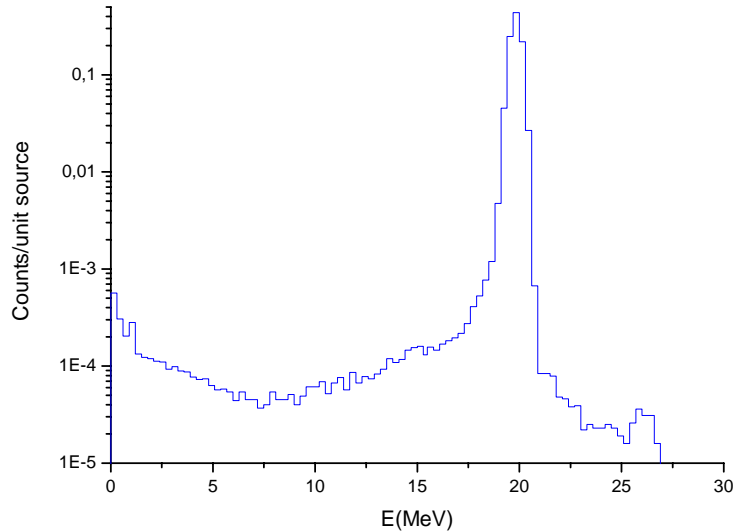


Fig. 35: Energy spectrum of LYSO for 30MeV protons.

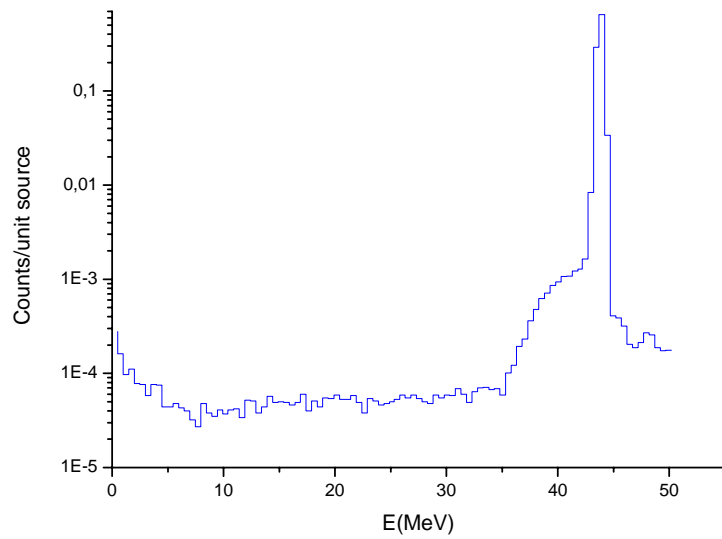


Fig. 36: Energy spectrum of LYSO for 50MeV protons.

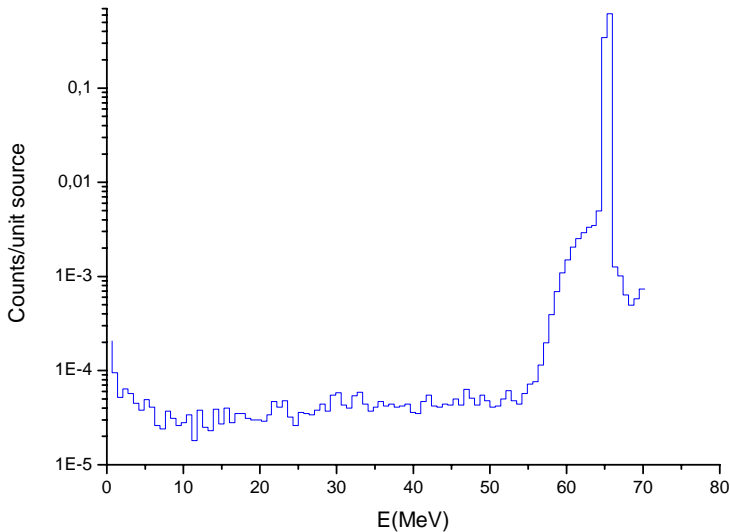


Fig. 37: Energy spectrum of LYSO for protons of 70MeV.

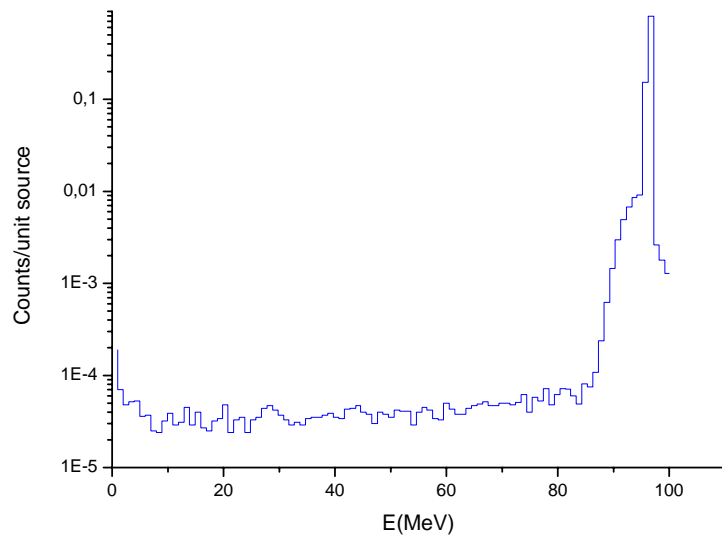


Fig. 38: Energy spectrum of LYSO for 100MeV protons.

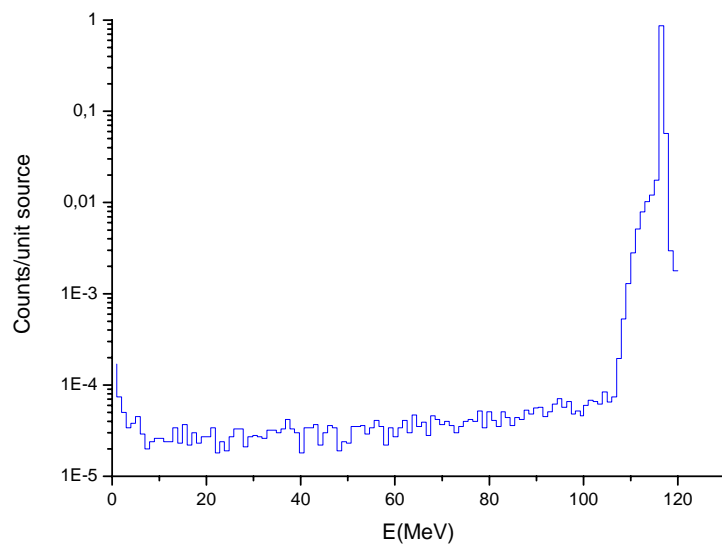


Fig. 39: Energy spectrum of LYSO for 120MeV protons.

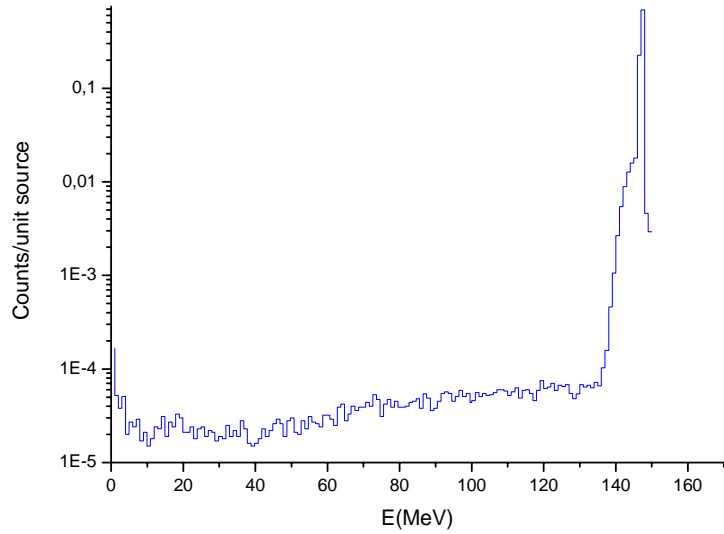


Fig. 40: Energy spectrum of LYSO for 150MeV protons.

VI-4 *The phoswich of (LaBr₃:Ce, LaCl₃:Ce) response*

The figures below show the energy spectra calculated by MCNPX code for the phoswich of BrillianceTM380 and BrillianceTM350 scintillators in the case of 120MeV and 150MeV proton energies.

Spectra of the protons of energy bellow than 100MeV are not represented because they have the same behaviour as the BrillianceTM380 spectra (all protons loose their energies inside LaBr₃:Ce).

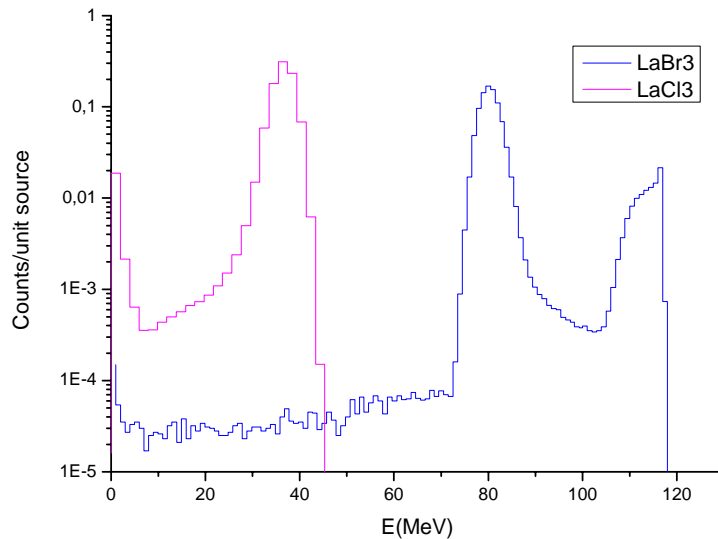


Fig. 41: Energy spectra for the LaBr₃ and LaCl₃ phoswich detector for 120MeV protons.

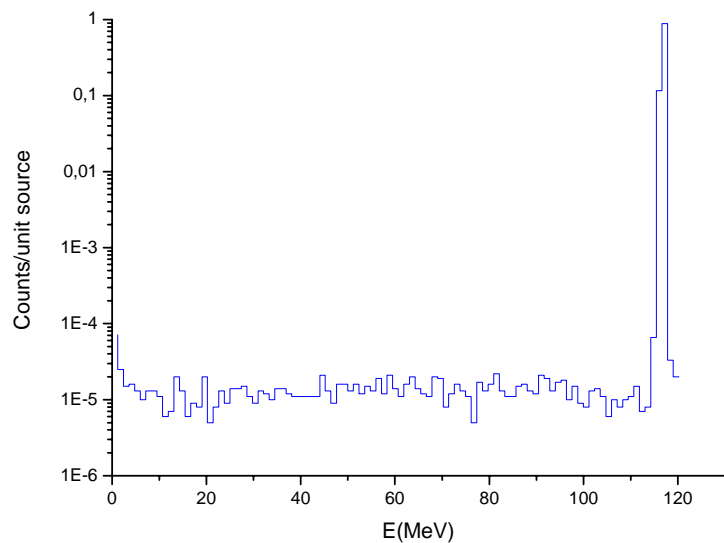


Fig. 42: The summed energy spectrum of LaBr₃ and LaCl₃ phoswich detector for 120MeV proton source.

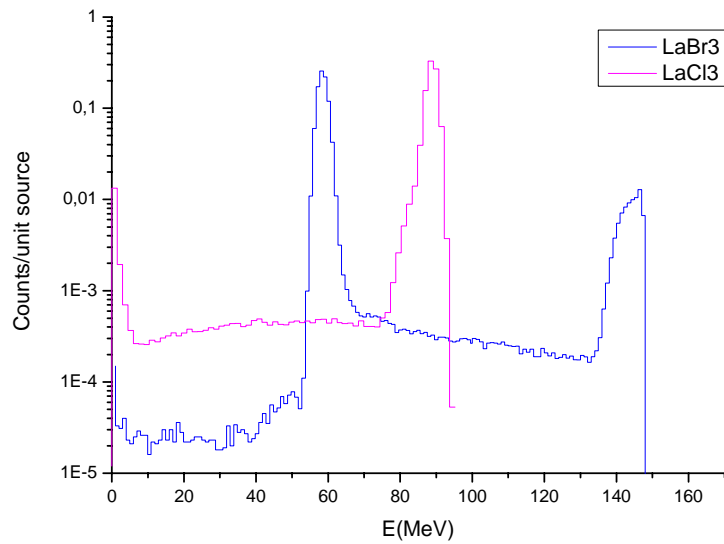


Fig. 43: Energy spectra for the LaBr₃ and LaCl₃ phoswich detector for 150MeV protons.

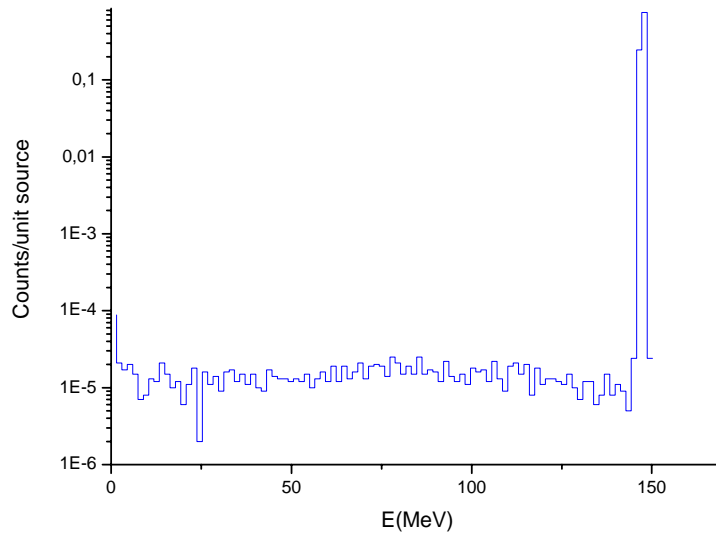


Fig. 44: The summed energy spectrum of LaBr₃ and LaCl₃ phoswich detector for 150MeV proton source.

VII- Conclusion

This study is focused on the analysis of a set of crystals response in order to select the best scintillators and to optimize the geometry of a double crystal phoswich detector for high energy photons and protons (up to 20MeV for photons and up to 150MeV for protons). For Photons, we have calculated the behaviour of peak to total efficiency versus incident energy and the energy spectra. In the case of protons, the study was focused on calculating the total energy deposition in each crystal and the extraction of the energy deposition spectra.

IX-References

- [1]: Denise B. Pelowitz, April 2005, “MCNPX USER’S MANUAL version 2.5”, LA-UR-05-2675, Los Alamos National laboratory (LANL), USA.
- [2]: C. M. Rozsa, Peter R. Menge, and M. R. Mayhugh, October 2007, “BrillanCe™ Scintillators (Performance Summary)”, Scintillation Products Technical Note, Saint-gobain detectors.